Kinetic Studies on the Reactions of Electrogenerated 9,10-Diphenylanthracene Cation Radical with Water and Alcohols by Means of Column-Electrolytic Stopped-Flow Method

Munetaka OYAMA, Koichi NOZAKI, Tsutomu NAGAOKA,† and Satoshi OKAZAKI*
Department of Chemistry, Faculty of Science, Kyoto University, Sakyo-ku, Kyoto 606
(Received May 25, 1989)

The reactions of 9,10-diphenylanthracene cation radical ($DPA^{+\cdot}$) with water and alcohols in acetonitrile (AN) were studied using a novel column-electrolytic stopped-flow spectrophotometric method. The reaction was first-order with respect to $DPA^{+\cdot}$ in all reactions. The reaction orders of other reactants were determined by plotting the logarithms of the apparent first-order rate constants (k_{app}'s) against the logarithms of the concentration of reactants. The plot of log k_{app} vs. log [alcohols] was linear, and hence the reaction was clearly determined to be second-order. On the other hand, the log k_{app} vs. log [water] plot did not show a linear relationship. Similar results were obtained in the reactions of 9,10-dimethylanthracene cation radical with water and methanol. Comparing the results obtained with water and alcohols, and considering the changes in the physicochemical properties of the AN–water medium, it was concluded that the reaction of water was second-order, though it had been believed previously to be first-order. Products of the reactions are *trans*- and *cis*-9,10-dialkoxy-9,10-diphenyl-9,10-dihydroanthracene in many cases.

During the last two decades, much attention has been devoted to the reactions of electrogenerated organic cation radicals. Complicated mechanisms and kinetics of reactive intermediates in the anodic oxidation processes of organic compounds have gradually become apparent.[1,2]

In these studies, most workers used electrochemical methods such as chronoamperometry, cyclic and linear sweep voltammetry, the rotating disk electrode method, and/or electrospectrochemical methods with an optically transparent electrode.[3] However, it is not easy to analyze unknown reactions of cation radicals by those methods. The difficulties in the kinetic studies generally result from the characteristics of the electrode process as follows: (1) Heterogeneous reactions occur in the vicinity of the electrode surface. (2) Successive reactions in the diffusion layer involve some EC processes.

If the objective cation radical is stable enough to permit being transferred from the electrolytic cell to the optical cell, its reactions with nucleophiles can be analyzed as homogeneous ones, separately from any influences of electrode conditions such as electrode potentials and adsorption etc.[4] Evans and Blount applied the stopped-flow technique to the analyses of the reactions of 9,10-diphenylanthracene (DPA) cation radical ($DPA^{+\cdot}$) with various nucleophiles in acetonitrile (AN).[5,6] In their experiment, the electrolyzed solution containing $DPA^{+\cdot}$ was delivered via a closed system to a reservoir in the stopped-flow apparatus. Therefore, unstable electrogenerated species, whose life-times were less than ten seconds, were difficult to examine.

For the purpose of investigating the reactions of less stable electrogenerated species (ca. <1 s), we have developed a column-electrolytic stopped-flow spectrophotometric method, in which a column-electrolytic flow cell was set up between a reservoir and a jet mixer in a stopped-flow spectrophotometer. In the present work, for the evaluation of a novel method, the reactions of $DPA^{+\cdot}$ with water and alcohols (ROH) have been analyzed.

The reaction of $DPA^{+\cdot}$ with water has been studied using several techniques; the spectroscopic method,[4] by means of an optically transparent thin layer electrode[7,8] and the stopped-flow method.[5] In the present work, we have studied the reactions of $DPA^{+\cdot}$ not only with water but also with alcohols concurrently, in order to compare these reactions. In addition, the reactions of the 9,10-dimethylanthracene (DMA) cation radical ($DMA^{+\cdot}$) have been investigated.

Experimental

Apparatus. Figure 1 shows the schematic diagram of the column-electrolytic stopped-flow spectrophotometer. The solution containing parent molecules and supporting electrolytes is stored in one reservoir and the reactant solution containing the nucleophile is stored in the other side. After the cation radicals are generated in the electrolytic cell, the electro-oxidized solution is rapidly mixed with the reactant solution by pressurizing with nitrogen gas (5 kg cm^{-2}).

For slow reactions as those in the present work, in which the half-life was longer than 0.5 s, only one line assembly was used in order to avoid the temperature change caused by mixing of the solvents. In this mode, the sample solution containing both parent molecules and the nucleophile was stored in one reservoir. Immediately after electro-oxidizing the solution, the cation radical generated was sent directly to an optical flow cell.

Figure 2 shows the cross-sectional view of the flow electrolytic cell. Carbon wool (CW) packed tightly inside a microporous glass diaphragm tube (PGT; i.d. 8 mm, l. 40 mm) acts as the working electrode. The carbon wool was

† Present address: Department of Applied Chemistry, Faculty of Engineering, Yamaguchi University, Tokiwadai 2577, Ube 755.

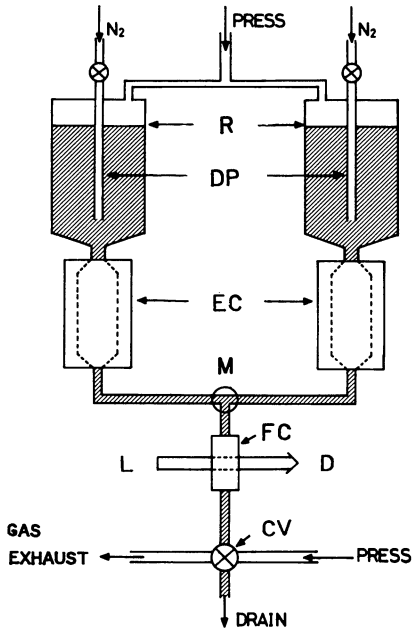

Fig. 1. Schematic diagram of the column-electrolytic stopped-flow spectrophotometer. R, reservoir. DP, deoxygenating pipe. EC, electrolytic cell. M, mixer. FC, flow cell. L, light beam. D, photo-detector. CV, control valve.

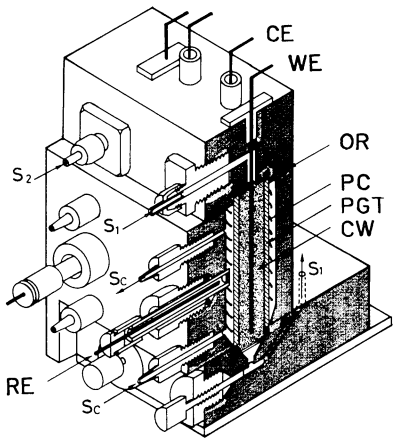

Fig. 2. Cross-sectional view of the column-electrolytic cell. WE, platinum lead wire to working electrode. CE, platinum lead wire to counter electrode. RE, reference electrode. OR, O-ring. PC, platinum coil counter electrode. PGT, porous glass tube. CW, carbon wool working electrode. S_1, S_2, sample solution. S_c, counter solution.

in contact electrically with a platinum lead wire (WE). Owing to the large surface area of the carbon wool against the sample volume, large amounts of cation radicals can be easily generated for a short time. Hence, in this study, cation radicals were generated with controlled potential pulse electrolysis for 1 s. Electrolytic efficiencies are described in the following section. The pulse electrolysis was carried out with a PAR Model 173 Potentiostat. The electrolysis currents were ca. 10—50 mA and the solution resistance was compensated using a PAR Model 179 Module.

Time changes in absorbance at a fixed wavelength were measured by a photomultiplier (PM). The time decay profile was acquired as a set of 500 digital data points. Procedures such as pulse electrolysis, flow control of the solution and data acquisition were performed by a microcomputer, DEC LSI-11/23. The operation of stopped-flow and the optical observation were carried out by the Union Giken RA 702 stopped-flow spectrophotometer.

All measurements were carried out at 25±0.5 °C using a thermostat, Coolnics Model CTR-120.

Reagents. 9,10-Diphenylanthracene (Nacalai Tesque, GR grade) was purified on a silica-gel column with benzene as eluent and was then recrystallized twice from AN–chloroform. 9,10-Dimethylanthracene (Tokyo Kasei, GR grade) was recrystallized twice from methanol. Acetonitrile (Wako, GR grade) was distilled twice over P_2O_5. Tetraethylammonium perchlorate (TEAP) was prepared by adding tetraethylammonium bromide to a solution of sodium perchlorate, and was recrystallized four times from water. It was dried over P_2O_5 in vacuo at 80 °C one night before use. Water was purified by a Milli-Q system. Alcohols (Wako, GR grade) were used without further purification.

Kinetic Analysis—Reaction Order Analysis. In kinetic analysis of complex reactions, it is significant to determine the reaction order of each species. The reaction order is generally a constant value, but sometimes it varies with concentration.[9] Hence, it is effective first to determine the reaction order from differential equations.

In the reaction of $DPA^{+\cdot}$ with ROH, the differential rate is presumed to be expressed as follows:

$$-\mathrm{d}[DPA^{+\cdot}]/\mathrm{d}t = k[DPA^{+\cdot}]^p[DPA]^q[ROH]^r[H^+]^s \quad (1)$$

where p, q, r, and s denote the reaction orders of each species, $DPA^{+\cdot}$, DPA, ROH, H^+, respectively. Equation 1 was then written in its logarithmic form.

$$\log(-\mathrm{d}[DPA^{+\cdot}]/\mathrm{d}t) = \log k + p\log[DPA^{+\cdot}] + q\log[DPA] + r\log[ROH] + s\log[H^+] \quad (2)$$

According to Eq. 2, the reaction order of $DPA^{+\cdot}$ can be determined from the slope of the plot of log $(-\mathrm{d}[DPA^{+\cdot}]/\mathrm{d}t)$ vs. log $[DPA^{+\cdot}]$ under the conditions that the concentrations of the other species are kept constant.

Once the reaction order of $DPA^{+\cdot}$ is determined, Eq. 1 is expressed as below using the apparent rate constant, k_{app},

$$-\mathrm{d}[DPA^{+\cdot}]/\mathrm{d}t = k_{app}[DPA^{+\cdot}]^p \quad (3)$$

where

$$k_{app} = k[DPA]^q[ROH]^r[H^+]^s. \quad (4)$$

In its logarithmic form,

$$\log k_{app} = \log k + q\log[DPA] + r\log[ROH] + s\log[H^+]. \quad (5)$$

According to Eq. 5, the reaction order of each species can be obtained by plottint log k_{app} vs. logarithmic concentration of each species.

Product Analysis. Product analysis was carried out using

batchwise constant potential electrolysis for the reactions with water, methanol, ethanol, 1-propanol, and 1-butanol. The AN solution of 100 ml containing 1 mM (1 M=1 mol dm^{-3}) DPA and 0.1 M TEAP was brought into the anodic chamber of an H-type electrolytic cell and then 1 M water or alcohol was added to the solution. The solution was electro-oxidized using a platinum mesh working electrode at the constant potential of +0.95 V vs. Ag/Ag^+ in AN until the electrolysis current decreased almost to zero. The solution was evaporated to ca. 10 ml. It was poured into water (100 ml) and extracted with benzene. The benzene extract was evaporated and the residue was separated on a silica-gel column with benzene as eluent. The products were identified by melting point measurements, NMR and MS.

Results

1. Electrolytic Efficiencies. a) Reduction of Ferricyanide in an Aqueous Solution Containig 0.5 M KCl: The electrolytic cell in this system was designed to utilize the capability of column-electrolysis, which allows quantitative oxidation or reduction of substances in a short period of time.

Figure 3 shows the plot of the concentration of ferricyanide ($Fe(CN)_6^{3-}$), which was determined from the absorbance at 436 nm ($\varepsilon_{Fe(CN)_6^{3-}}$=743), after an electrolysis of 1.0 mM $Fe(CN)_6^{3-}$ at various potentials for 1 s. The $Fe(CN)_6^{3-}$ solution could be electrolyzed quantitatively to ferrocyanide ($Fe(CN)_6^{4-}$) even in such a short time. In addition, the plot of the natural logarithms of $[Fe(CN)_6^{3-}]/[Fe(CN)_6^{4-}]$ against the applied potentials showed a good relationship as expected from the Nernst's equation,

$$E = E^\circ + \frac{RT}{F} \ln \frac{[Fe(CN)_6^{3-}]}{[Fe(CN)_6^{4-}]}. \quad (6)$$

The number of electrons involved in this electrode process was determined to be 1.0 from the slope of the plot, which also confirms that quantitative electrolysis could be achieved within 1 s in a low resistance medium.

b) Oxidation of DPA in an AN Solution Containing 0.1 M TEAP: Secondary, the electrolysis efficiency in the present system, namely the oxidation of DPA in AN containing 0.1 M TEAP, was examined. Figure 4 shows the dependence of the absorbance of $DPA^{+\cdot}$ on the applied potential in this electrolytic method, with the cyclic voltammogram of DPA. The half-wave potential ($E_{1/2}$) in the cyclic voltammogram was 0.83 V, and the potential at half absorbance value was 0.85 V. Hence, the solution was electrolyzed properly under the controlled potential. As shown in this figure, the concentration of cation radicals can be controlled by changing the applied potential, which is one of the advantages of the present method. The

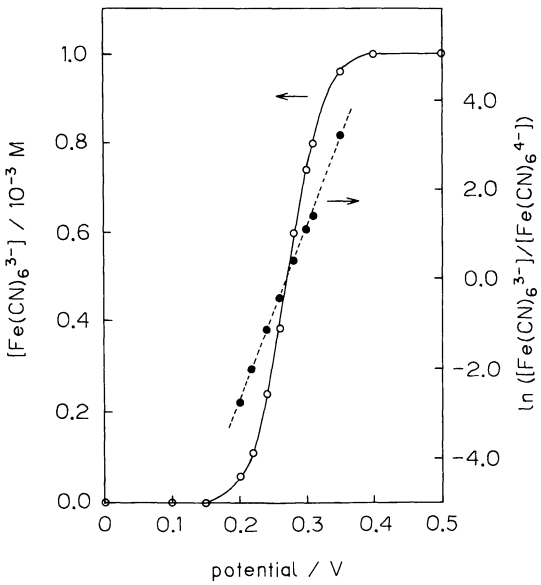

Fig. 3. Electrolytic efficiency in the reduction of 1.0×10^{-3} M $Fe(CN)_6^{3-}$ in aqueous solution containing 0.5 M KCl. The electrolyzed solution was rapidly delivered into the optical flow cell after the pulse electrolysis for 1 s. Potential is versus Ag/AgCl. Initial potential: 0.6 V. (○) Potential vs. concentration of $Fe(CN)_6^{3-}$ plot. The absorbance at 436 nm was measured and transferred to the concentrtion. (●) Nernst's plot (potential vs. $\ln[Fe(CN)_6^{3-}]/[Fe(CN)_6^{4-}]$).

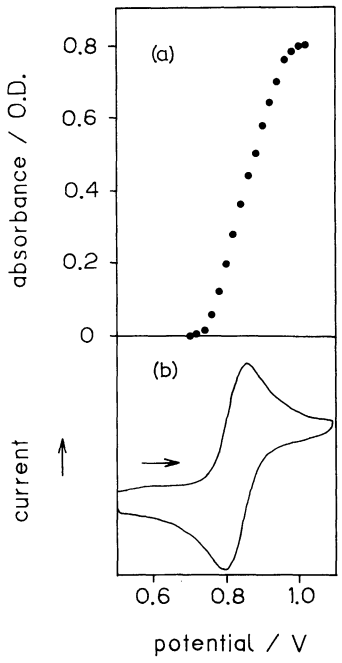

Fig. 4. Electrolytic efficiency in the oxidation of 5.0×10^{-4} M DPA in AN containing 0.1 M TEAP. (a) Dependence of the absorbance of $DPA^{+\cdot}$ at 653 nm on the applied potential. The electrolyzed solution was rapidly delivered into the optical flow-cell after the pulse-electrolysis for 1 s. Potential is versus Ag/Ag^+. Initial potential: 0.5 V. Light path: 2 mm. (b) Cyclic voltammogram of DPA measured at the scan rate of 0.1 V s^{-1} with Pt disk electrode (d. 0.5 mm). Potential is versus Ag/Ag^+.

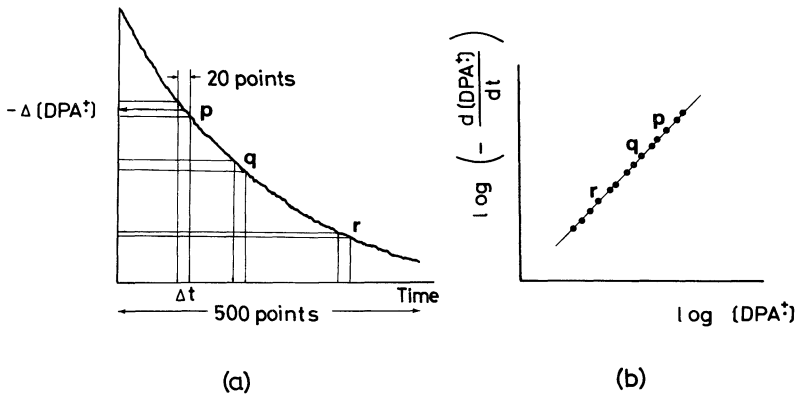

Fig. 5. Outline of data processing procedure. $-\Delta[DPA]^{+\cdot}/\Delta t$ and $[DPA^{+\cdot}]$ at each time were calculated as shown in the left figure. Regarding $-\Delta[DPA]^{+\cdot}/\Delta t$ as $-d[DPA]^{+\cdot}/dt$, the reaction order of $DPA^{+\cdot}$ was determined by the slope of the plot, $\log(-d[DPA]^{+\cdot}/dt)$ vs. $\log[DPA^{+\cdot}]$, in the right figure.

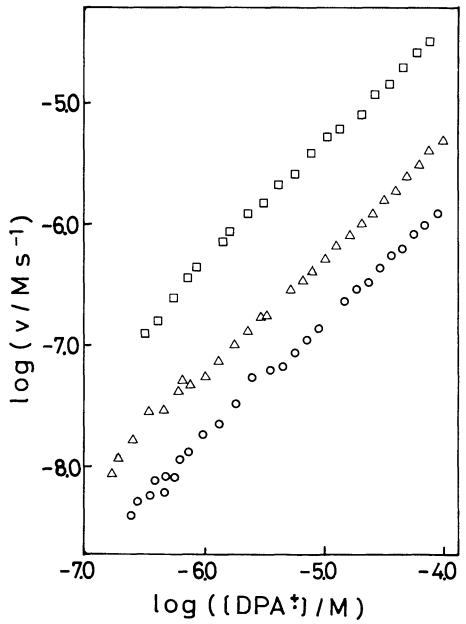

Fig. 6. Dependence of $-d[DPA^{+\cdot}]/dt$ on $[DPA^{+\cdot}]$ in the reaction of $DPA^{+\cdot}$ with water. C_{DPA} 5×10^{-4} M, TEAP 0.1 M, H_2O 0.35 M (○), 1.0 M (△), 5.0 M (□) in AN. In this figure, v represents $-d[DPA^{+\cdot}]/dt$.

maximum concentration was calculated to be ca. 4.6×10^{-4} M using the molar excitation coefficient value reported by Grant et al.[7] ($\varepsilon=8.75\times10^3$ at 653 nm), and therefore it was found that the solution containing ca. 90% $DPA^{+\cdot}$ can be delivered to the optical cell in this method.

2. Reactions of $DPA^{+\cdot}$ with Water and Methanol. a) Reaction Orders of $DPA^{+\cdot}$ and DPA: Since the time decay curve of absorbance was acquired as 500 data points, $-d[DPA^{+\cdot}]/dt$ was calculated using the linear approximation for every 20 data points as illustrated in Fig. 5a. Then, by displacing the data position, $\log(-d[DPA^{+\cdot}]/dt)$ was plotted against $\log[DPA^{+\cdot}]$ (Fig. 5b).

Figure 6 shows the relationships between $\log(-d[DPA^{+\cdot}]/dt)$ and $\log[DPA^{+\cdot}]$ in the reaction with water. The slopes of their plots for three different water concentrations ranged from 0.94 to 0.97. In the reaction with methanol shown in Fig. 7, the slopes were 0.91 and 0.95 for 1.0 M and 5.0 M methanol, respectively. The slopes of these plots for the other conditions were almost unity for both reactions. Accordingly it can be presumed that the reaction order of $DPA^{+\cdot}$ is unity (i.e. $p=1$ in Eq. 2) in both reactions.

However, the apparent reaction order of $DPA^{+\cdot}$ may be affected by the concentration of DPA.**

We therefore measured the time decay curves of

** In a strict treatment, the reaction order of $DPA^{+\cdot}$ can not be exactly determined by $\log(-d[DPA^{+\cdot}]/dt)$ vs. $\log[DPA^{+\cdot}]$ plot because of the low solubility of DPA in AN; the concentration of DPA was not high enough in comparison with the amount of DPA regenerated during the reaction.

Defining the concentration of dissolved DPA in the solution as C_{DPA}, the concentration of electrogenerated $DPA^{+\cdot}$ at $t=0$ as $[DPA^{+\cdot}]_0$, and that of DPA at that time as $[DPA]_0$, $C_{DPA}=[DPA]_0+[DPA^{+\cdot}]_0$. Based on the stoichiometry, $2DPA^{+\cdot}+2ROH \longrightarrow DPA(OR)_2+DPA+2H^+$, $[DPA]=[DPA]_0+([DPA^{+\cdot}]_0-[DPA^{+\cdot}])/2$. Hence, the following equation is obtained.

$$[DPA] = C_{DPA} - ([DPA^{+\cdot}]_0+[DPA^{+\cdot}])/2$$

Therefore, Eq. 2 must be rewritten as Eq. 2′, under the conditions that the concentrations of other species and $[DPA^{+\cdot}]_0$ are kept constant.

$$\log(-d[DPA^{+\cdot}]/dt) = \log k + p\log[DPA^{+\cdot}] + q\log(C_{DPA} - [DPA^{+\cdot}]/2 - \text{const}) + \text{const} \quad (2')$$

This equation indicates that if q is not equal to zero, it is not easy to determine the reaction orders.

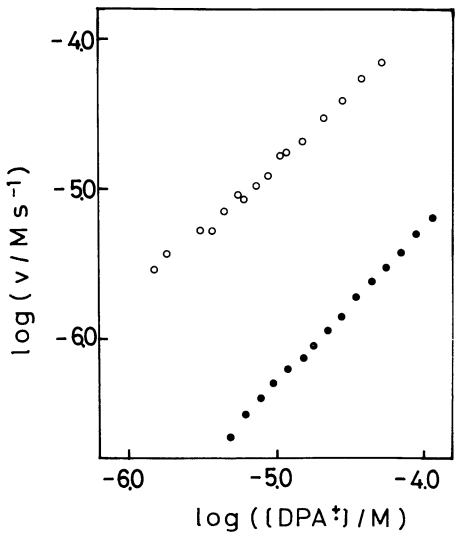

Fig. 7. Dependence of $-d[DPA^{+\cdot}]/dt$ on $[DPA^{+\cdot}]$ in the reaction of $DPA^{+\cdot}$ with methanol. C_{DPA} 5×10^{-4} M, TEAP 0.1 M, methanol 1.0 M (●), 5.0 M (○) in AN. In this figure, v represents $-d[DPA^{+\cdot}]/dt$.

$DPA^{+\cdot}$ when 5×10^{-5}, 1×10^{-4}, 2×10^{-4}, and 5×10^{-4} M DPA were dissolved, under the conditions that the concentrations of the other species and the initial concentration of $DPA^{+\cdot}$ were kept constant. The results showed that the concentration of DPA had no influence on the reaction rates. Thus, it is concluded that DPA is independent of the rate laws of both reactions, while $DPA^{+\cdot}$ has the first-order dependence on them (i.e., $p=1$ and $q=0$ in Eq. 2).

Since the reaction order of $DPA^{+\cdot}$ was unity in all of the reactions examined, the other reaction orders could be obtained readily with the apparent first-order rate constant, k_{app}.

$$-d[DPA^{+\cdot}]/dt = k_{app}[DPA^{+\cdot}] \qquad (3')$$

Thus, based on Eq. 5, the reaction order of each species was obtained by plotting log k_{app} vs. the logarithmic concentration of each species. The k_{app} value under particular conditions was determined from four runs. The k_{app} was calculated from absorbance vs. time curve using the phase-plane method.[10]

b) Reaction Order of H^+: The concentration of H^+ was varied from 10^{-5} M to 10^{-2} M for the reaction with water, and from 10^{-4}M to 10^{-2} M for the reaction with methanol by adding perchloric acid (70% aqueous solution) to the solution.[11] The concentration of water was corrected by subtracting the water contents in aqueous perchloric acid solution. In the reaction with methanol, however, a small amount of water (max. ca. 20 mM) coexisted.[12] The plot of log k_{app} vs. log$[H^+]$ in Fig. 8 shows that the rate law is independent of the concentration of H^+.

c) Reaction Orders of Water and Methanol: Figure 9 shows the plots of log k_{app} vs. log[ROH]. In the

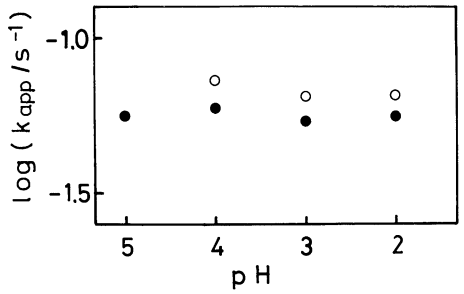

Fig. 8. Dependence of k_{app} on pH in the reactions of $DPA^{+\cdot}$ with water (●) and methanol (○). C_{DPA} 5×10^{-4} M, TEAP 0.1 M, water or methanol 1.0 M in AN.

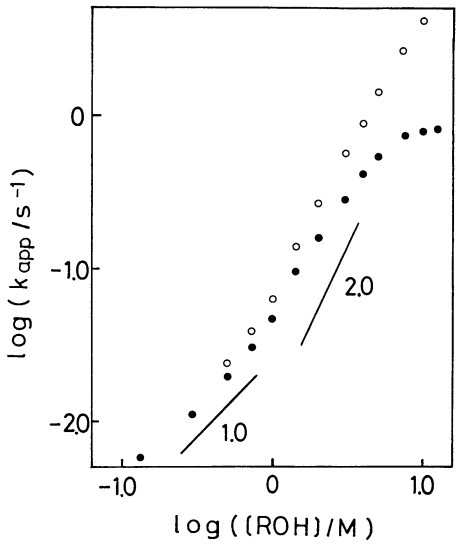

Fig. 9. Dependence of k_{app} on [ROH] in the reactions of $DPA^{+\cdot}$ with water (●) and methanol (○). C_{DPA} 5×10^{-4} M, TEAP 0.1 M, H_2O 0.12—15 M or methanol 0.5—10 M in AN.

reaction with methanol, a linear relationship was found in the concentration range from 0.5 M to 10 M; its slope was calculated to be 1.80 by the least squares method. Thus, the reaction order of methanol was determined to be second-order. With respect to the reaction with water, however, the reaction order varied with the water concentration (Fig. 9). The slope was 1.06 at water concentrations lower than 1 M, whereas it was 1.52 in the range from 1 M to 4 M and became zero over 5 M.

3. Reaction of $DPA^{+\cdot}$ with Other Alcohols. The reactions of $DPA^{+\cdot}$ with ethanol, 1-propanol, 2-propanol, 1-butanol, and 1-pentanol were also analyzed by this method. In all cases, the reaction order of $DPA^{+\cdot}$ was unity. Furthermore, like the reaction of $DPA^{+\cdot}$ with methanol, log k_{app} vs. log[ROH] plots exhibited a linear relationship. The slopes are summarized in Table 1 together with the k_{app}'s with 2 M of ROH. It was proved that the reaction order of ROH was second in all cases, although the slopes

Table 1. Kinetic Data in the Reactions of $DPA^{+\cdot}$ with Alcohols

Alcohol	Concentration range/M	Number of data points	Slope	k_{app}/s^{-1} [a] at 2.0 M
Methanol	0.5—10	10	1.80 (0.999)	0.26_5
Ethanol	0.5—10	10	1.81 (0.999)	0.15_9
1-Propanol	1.0—7.0	7	1.84 (0.998)	0.13_2
2-Propanol	2.0—7.0	5	1.68 (0.998)	0.019_1
1-Butanol	1.0—7.0	6	2.11 (0.999)	0.17_5
1-Pentanol	1.0—5.0	5	1.71 (0.992)	0.24_6

Parentheses indicate the correlation coefficients. a) Average value of four runs.

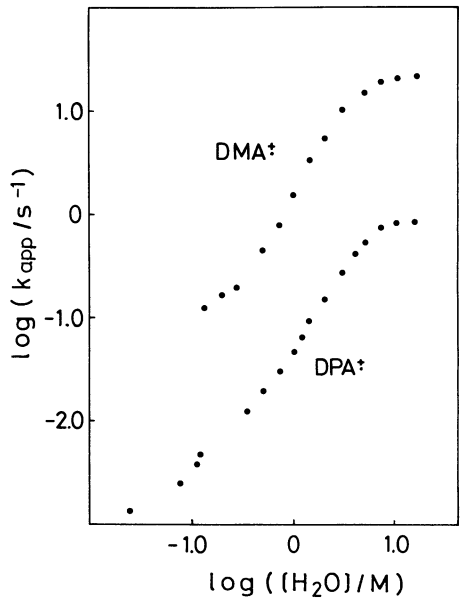

Fig. 10. Dependence of k_{app} on $[H_2O]$ in the reactions of $DPA^{+\cdot}$ and $DMA^{+\cdot}$ with water. C_{DPA} or C_{DMA} 5×10^{-4} M, TEAP 0.1 M, water 0.15—15 M (for $DPA^{+\cdot}$) in AN.

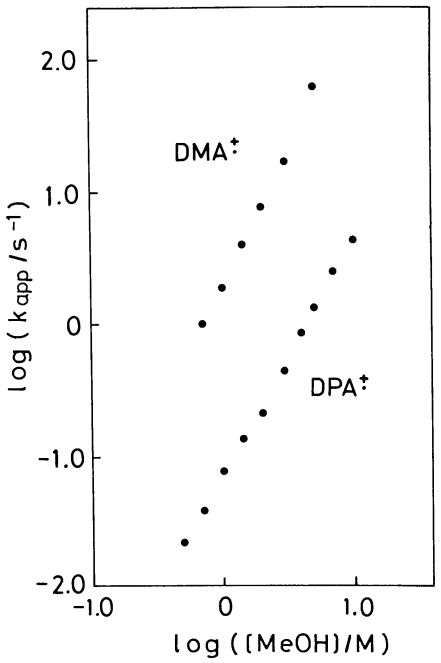

Fig. 11. Dependence of k_{app} on [MeOH] in the reactions of $DPA^{+\cdot}$ and $DMA^{+\cdot}$ with methanol. C_{DPA} or C_{DMA} 5×10^{-4} M, TEAP 0.1 M, methanol 0.7—5 M (for $DPA^{+\cdot}$) in AN.

slightly deviated from two.

On the reaction rates, there were no notable differences among alcohols, except 2-propanol. The reaction rate with 2-propanol was lower than those with the other alcohols examined. This is probably due to a steric effect.

4. Reactions of $DMA^{+\cdot}$. The kinetic study on the reaction of $DMA^{+\cdot}$ was also carried out. Figure 10 shows the plot of log k_{app} vs. $\log[H_2O]$ superimposed on the results of $DPA^{+\cdot}$. It is of interest that the reaction order plot exhibits a non-linear dependence similar to that of $DPA^{+\cdot}$. Furthermore, second-order dependence was observed in the reaction with methanol, as shown in Fig. 11.

5. Products in the Reactions of $DPA^{+\cdot}$ with ROH. From the NMR analysis, it was found that both *trans*- and *cis*-9,10-dialkoxy-9,10-diphenyl-9,10-dihydroanthracene, $DPA(OR)_2$ (**1**, **2**), were produced in three cases (R; H, CH_3, C_4H_9). In the case of water, trans and cis forms were separated using column chromatography with benzene as eluent. The melting points were 261 °C (263 °C in Ref. 13) for the trans form (**1a**) and 188 °C (195 °C in Ref. 13) for cis one (**2a**). In this case, some minor by-products were found

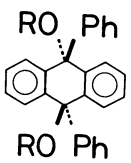

1a—e

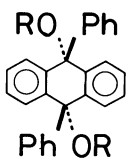

2a—e

a	R: H
b	CH_3
c	C_2H_5
d	C_3H_7
e	C_4H_9

by TLC. However, their amounts were so small that the species could not be identified.

In the reaction with water, ethanol and 1-propanol, trans and cis forms (**1**, **2**) were confirmed by NMR. It was found that the ratio of both forms were nearly 1:1. In the case of methanol and 1-butanol, however, the products were not dissolved completely in $CDCl_3$. Thus, it seems that only one form was detected by NMR. Thus the final products in the reactions with alcohols were also inferred to be *trans*- and *cis*-$DPA(OR)_2$.

Results of ^1H NMR ($CDCl_3$ and CD_3CN[14]) and MS measurements of the products were as follows:

(**a**) 9,10-Dihydroxy-9,10-dihydro-9,10-diphenylanthracene; δ=2.8, 3.3 (2H, s, OH), 7.0 (10H, m), 7.3 (4H, m), 7.6 (4H, m); *m/z*(rel intensity) 364(M^+; 0.7), 347(100), 330(19), 287(6), 271(19).

(**b**) 9,10-Dimethoxy-9,10-dihydro-9,10-diphenylanthracene; δ=3.2 (6H, s, OCH_3), 7.3—7.4 (10H, m), 7.4—7.5 (4H, m), 7.5—7.6 (4H, m); *m/z* (rel intensity) 392 (M^+; 0.5), 361(97), 330(100), 284(49).

(**c**) 9,10-Diethoxy-9,10-dihydro-9,10-diphenylanthracene; δ=1.1, 1.2 (6H, t, J=6 Hz,$C\underline{H}_3CH_2O$), 3.0, 3.3 (4H, q, J=6 Hz, $CH_3C\underline{H}_2O$), 7.2—7.6 (18H, m).

(**d**) 9,10-Dipropoxy-9,10-dihydro-9,10-diphenylanthracene; δ=0.9 (6H, t, J=10 Hz, $C\underline{H}_3CH_2CH_2O$), 1.5—1.7 (4H, m, $CH_3C\underline{H}_2CH_2O$), 2.9, 3.3 (4H, t, J=9 Hz, $CH_3CH_2C\underline{H}_2O$), 7.2—7.6 (18H, m).

(**e**) 9,10-Dibutoxy-9,10-dihydro-9,10-diphenylanthracene; δ=0.9 (6H, t, J=10 Hz, $C\underline{H}_3CH_2CH_2CH_2O$), 1.5—1.7 (8H, m, $CH_3C\underline{H}_2C\underline{H}_2CH_2O$), 3.2 (4H, t, J=8 Hz, $CH_3CH_2CH_2C\underline{H}_2O$), 7.5—7.6 (18H, m).

Discussion

Reaction Mechanisms. It was clearly concluded, from the results, that the reactions of $DPA^{+\cdot}$ with alcohols are first-order in $DPA^{+\cdot}$ and second-order in alcohols. That is, the rate law can be expressed by Eq. 7.

$$-d[DPA^{+\cdot}]/dt = k[DPA^{+\cdot}][ROH]^2 \quad (7)$$

This rate law can be explained if the first step (Eq. 8) in Scheme 1 is in equilibrium and the proton abstraction by another alcohol molecule (Eq. 9) is the rate determining step (rds). The k is represented as $2K_1k_2$ using the steady state approximation on $DPA(OR)^{\cdot}$ and $DPA(OR)^+$.

$$DPA^{+\cdot} + ROH \underset{}{\overset{K_1}{\rightleftharpoons}} DPA(ROH)^{+\cdot} \quad (8)$$

$$DPA(ROH)^{+\cdot} + ROH \xrightarrow[\text{rds}]{k_2} DPA(OR)^{\cdot} + ROH_2^+ \quad (9)$$

$$DPA(OR)^{\cdot} + DPA^{+\cdot} \longrightarrow DPA(OR)^+ + DPA \quad (10)$$

$$DPA(OR)^+ + 2ROH \longrightarrow DPA(OR)_2 + ROH_2^+ \quad (11)$$

Scheme 1.

On the other hand, in the case of the reaction of $DPA^{+\cdot}$ with water, our results emphasized the complex characteristics of the reaction; the reaction order of water varied depending on its concentration.

In the previous works, the reaction order of water was estimated to be first from the limited experimental range of the water concentration from 5×10^{-3} M to 1.50 M,[5] or from 2.5 M to 4 M.[8] The proposed mechanism was as follows:[5,8]

$$DPA^{+\cdot} + H_2O \xrightarrow[\text{rds}]{k_1} DPA(H_2O)^{+\cdot} \quad (12)$$

$$DPA(H_2O)^{+\cdot} + H_2O \rightleftharpoons DPA(OH)^{\cdot} + H_3O^+ \quad (13)$$

$$DPA(OH)^{\cdot} + DPA^{+\cdot} \longrightarrow DPA(OH)^+ + DPA \quad (14)$$

$$DPA(OH)^+ + 2H_2O \longrightarrow DPA(OH)_2 + H_3O^+ \quad (15)$$

Scheme 2.

where the first step is the rate determining step and the second is in equilibrium.

This discrepancy does not result from a fault in our method. That is because apparent deviations from a straight line can also be seen in the plot of k_{app} vs. water concentration in the previous works,[4,7] though it was not commented on. In addition, the k_{app} values over the above water concentration range are almost equal to those reported.

In order to explain the extraordinary relationship obtained only in water, the difference in the state of water and alcohols in AN must be considered. The fact that the reaction rate is independent of the sort of cation radicals (Figs. 10 and 11) also suggest the contribution of a medium effect.

The hydrogen-bond formation between AN and water or alcohols is well characterized by IR. On alcohols, the solute–nitrile interactions are stronger than the solute–solute interactions, so that methanol retains in the monomer state at concentrations up to 4 M.[15] By contrast, water exists in the form of 1:1 and 1:2 AN–water complexes depending on the concentration,[16] because the interactions between water molecules in AN are fairly large. Previous studies on the AN–water mixture by conductivity measurements[17,18] and NMR[19] also indicate that a high concentration water over 1 M tends to form higher-ordered structures (i.e., dimer and trimer forms). The nucleophilicity of the polymerized water molecule is probably less than that of the monomer because the reaction site is occupied by the hydrogen bonding. Consequently, the structural complexity in the AN–water mixed medium seems to bring about the extraordinary dependence of log k_{app} on log $[H_2O]$.[20]

It is, however, difficult to evaluate the state of water in AN quantitatively at each concentration in Fig. 9. Hence, we attempted to correct the reactivities of water

by adopting the activity coefficient. In general, the activity coefficient of the solute in a mixed solvent can be calculated from the vapor pressure, so that the activity coefficient of water in an AN–water mixture (f) at each concentration was estimated from the vapor pressure curve reported previously,[21] on the basis that f=1 for pure water. With f, Eq. 4 is rewritten by Eq. 16 taking into consideration the above results of q=s=0,

$$k_{app} = .k(f[H_2O])^r \quad (16)$$

and its logarithmic form,

$$\log k_{app} = \log k + r\log(f[H_2O]). \quad (17)$$

Figure 12 shows the plot of log k_{app} vs. log(f[H_2O]). It should be noted that the reaction order of water became approximately second, while it was curved upwards at the lower water concentration range.

In the kinetic measurement at the water concentrations, it is necessary to take into account side reactions, which were also suggested from the results of product analysis by TLC though the products could not be specified. For example, nearly 10% $DPA^{+\cdot}$ decayed for 60 s in AN to which no water was added, in comparison the half-life of $DPA^{+\cdot}$ is 65 s in 0.5 M H_2O. With decreasing water concentration, side reactions will become significant, and the k_{app}'s obtained in the low water concentration range contain some positive errors. This seems to be the reason why the corrected plots were curved upwards at the lower concentration range.

From the above discussion and compared with the results obtained in alcohols, the mechanism of the reaction of $DPA^{+\cdot}$ with water is substantially the same as that with alcohols (Scheme 1) and its rate law should be expressed by Eq. 7.

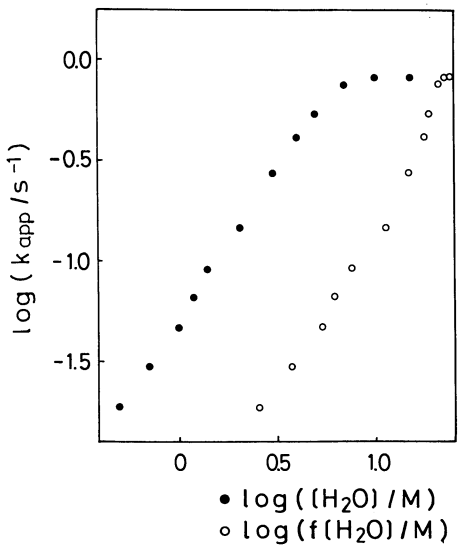

Fig. 12. Activity correction for log (k_{app}/s^{-1}) vs. log ([H_2O]/M) plot in the reaction of $DPA^{+\cdot}$ with water.

Reaction Products. Our results on the reaction products are also in conflict with the previous report. Sioda reported that the final product in the reaction of $DPA^{+\cdot}$ with water was *trans*-$DPA(OH)_2$.[4] In the present study, however, *cis*-$DPA(OH)_2$ was also found to be produced.

Considering the reaction mechanism, $DPA(OH)^+$ is produced as an intermediate and reacts rapidly with water. Then, it seems reasonable to assume that both forms are produced at the same time.

Comparison with the Reactions of Other Cation Radicals. The reactions of other cation radicals with water have been extensively investigated, although no kinetic studies with alcohols have been reported.

In the reaction of the thianthrene cation radical ($TH^{+\cdot}$) with water, many investigations were made and a complex mechanism has been revealed.[22] In this case as well, the first stage of the reaction, namely, the encounter of $TH^{+\cdot}$ with water, was found to be in equilibrium, though the subsequent processes were more complex than those of $DPA^{+\cdot}$. Furthermore, a similar mechanism was also proposed on the reaction of 10-phenylphenothiazine (PPTZ) dication ($PPTZ^{2+}$) with water.[23] The results showed that the rate was expressed as Eq. 18.

$$-d[PPTZ^{2+}]/dt = k[PPTZ^{2+}][H_2O]^2 \quad (18)$$

The first step, the encounter of $PPTZ^{2+}$ with water, is in equilibrium and the second step, in which a proton is abstracted by another water molecule, is rate determining.

Comparing these reactions, it appeared to be reasonable that Eq. 12 is in equilibrium in the reaction mechanism of $DPA^{+\cdot}$ with water.

Conclusion

Though the reaction of $DPA^{+\cdot}$ with water had been thought to be first-order in both $DPA^{+\cdot}$ and water, it has been established in this study that the reaction scheme is expressed by Eqs. 8—11, which is the same mechanism as that for alcohols. It is important to pay particular attention to the changes in the physicochemical properties of the medium, especially in the reaction with water. Our results indicate that the reaction of cation radicals with methanol can be regarded as a model reaction for that with water.

In the present study, the reaction order of the cation radical was unity over a wide concentration range and under all experimental conditions. The column-electrolytic stopped-flow method will be useful for the analyses of more complex reactions of electrogenerated intermediates. Furthermore, this method can be applied to the analyses of unstable electrogenerated ion radicals with half-lives as short as 100 ms. These studies are under way and will be published elsewhere.

The authors wish to thank Dr. Shotaro Oka of the Central Institute of Shimadzu Manufacture Co., for his kind support in constructing the column electrolysis cell.

This work was supported in part by a Grant-in-Aid for Scientific Research No. 63470029 from the Ministry of Education, Science and Culture.

References

1) K. Yoshida, "Electrooxidation in Organic Chemistry," Wiley, New York (1984).

2) O. Hammerich and V. D. Parker, *Adv. Phys. Org. Chem.*, **20**, 55 (1984).

3) A. J. Bard and L. R. Faulkner, "Electrochemical Method," Wiley, New York (1980).

4) R. E. Sioda, *J. Phys. Chem.*, **72**, 2322 (1968).

5) J. F. Evans and H. N. Blount, *J. Org. Chem.*, **41**, 516 (1976).

6) J. F. Evans and H. N. Blount, *J. Am. Chem. Soc.*, **100**, 4149 (1978).

7) G. C. Grant and T. Kuwana, *J. Electroanal. Chem.*, **24**, 11 (1970).

8) H. N. Blount and T. Kuwana, *J. Electroanal. Chem.*, **27**, 464 (1970).

9) M. Oyama, K. Nozaki, H. Hatano, S. Okazaki, and T. Nagamura, Proceedings of 172 nd Meeting of the Electrochemical Soc., Honolulu, Oct. 1987, Abstr., No. 1644.

10) J. R. Bacon and J. N. Demas, *Anal. Chem.*, **55**, 653 (1983).

11) Concentration of H^+ was calculated under the assumption that perchloric acid is completely dissociated in these media.

12) In our purification, AN contained 10—20 mM water.

13) Ch. Pinazzi, *Ann. Chim. (Paris)*, **7**, 397 (1962).

14) Only for **1a** and **2a**. In this case, $CDCl_3$ could not be used due to the poor solubility.

15) S. S. Mitra, *J. Chem. Phys.*, **36**, 3286 (1962).

16) O. D. Bonner and Y. S. Choi, *J. Phys. Chem.*, **78**, 1723 (1974).

17) W. S. Muney and J. F. Coetzee, *J. Phys. Chem.*, **66**, 89 (1962).

18) M. I. Chantooni, Jr. and I. M. Kolthoff, *J. Am. Chem. Soc.*, **89**, 1582 (1967).

19) A. J. Easteal, *Aust. J. Chem.*, **32**, 1379 (1979).

20) Another reason is presumed to be the drastic change in chemical properties of the medium. For example, dielectric constants of AN, water and methanol are 36.0, 78.6, 32.6, respectively. Therefore, the dielectric constant of AN–water mixture changes widely depending on the water content.

21) V. de Landsberg, *Bull. Soc. Chim. Belg.*, **49**, 59 (1940).

22) V. D. Parker, *Acc. Chem. Res.*, **17**, 243 (1984).

23) K. Yasukouchi, I. Taniguchi, H. Yamaguchi, J. Ayukawa, K. Ohtsuka, and Y. Tsuruta, *J. Org. Chem.*, **46**, 1679 (1981).